

ULTRASOUND IMAGING OF STIFFNESS WITH TWO FREQUENCY PULSES

ANDZEJ NOWICKI, MICHAŁ BYRA, JERZY LITNIEWSKI,
JANUSZ WÓJCIK

Institute of Fundamental Technological Research, Polish Academy of Sciences
Pawińskiego 5b, Warsaw, Poland
mbyra@ippt.pan.pl

Nowadays there are new modalities in ultrasound imaging allowing better characterization of tissue regions with different stiffness. We are proposing a novel approach based on compression and rarefaction of tissue simultaneously with imaging. The propagating wave is a combination of two pulses. A low frequency pulse is expected to change the local scattering properties of the tissue due to compression/rarefaction while a high frequency pulse is used for imaging. Two transmissions are performed for each scanning line. First, with the imaging pulse that propagates on maximum compression caused by a low frequency wave. Next, the low frequency wave is inverted and the imaging pulse propagates over the maximum rarefaction. After the processing of the subtracted echoes from subsequent transmissions including wavelet transform and band-pass filtering, differential images were reconstructed. The low frequency wave has a visible impact on the scattering properties of the tissue which can be observed on a differential image.

INTRODUCTION

US imaging is based on the reflectivity of ultrasonic waves at the interfaces between tissue, differing in their acoustic impedances, being expressed by a product of density and longitudinal speed (depending on the modulus of elasticity).

The elasticity of materials describes their property to return to their original shape after the material has been subjected to an external force or distorting stress.

Tissue elasticity was, for a long time, estimated using manual palpation. In the process of palpation, physicians apply manual pressure to the patient's skin and in this way sense the location and stiffness of the organ in the body. Manual palpation, although widely used, has limitations. There is relatively easy access only to the superficial organs, while in more deeply located organs like the thyroid or liver the physician can only differentiate large masses with significantly different stiffness.

An excellent general review of the methods applied in elastography and historical survey of palpation techniques was made by Wells and Liang [1].

1. IMAGING USING NONLINEAR PROPAGATION

Standard US imaging has limited contrast dynamics and it is rather difficult to display very slight local changes in tissue properties. Some improvements can be obtained using the nonlinear behavior of the wave propagation in tissue. There are two relatively novel techniques enabling imaging of tissue regions with only a slight difference in density or the speed of sound. The first US modality, called Tissue Harmonic Imaging (THI), was first described by Averkiou [2]. Nowadays, this technique is routinely used in ultrasonic imaging proving its importance in improving the quality of grey-scale images, especially in the examining of the so-called “difficult patients” [3], [4]. However, it has to be stressed that this is far from optimal because only half of the available transducer bandwidth is used for image formation – the lower half for transmission and the upper half during reception. The importance of the reduced dynamic range and penetration encountered in THI was also pointed out [2], [5]. Since the images are formed with only the first harmonic components which are usually at least 20 dB below the fundamental, the dynamic range is limited. The nonlinear effects including contrast agents improving imaging sensitivity has been intensively studied by many authors [6], [7].

An improved resolution can be achieved with an imaging method called pulse inversion (PI). In contrast to conventional harmonic imaging, for pulse inversion imaging, the whole frequency spectrum can be used during reception. Alternate pulses, and radians out of phase, are transmitted along the same scan line [8]. The echoes received from the pair transmission are then added together to build up the final image line. This method removes the requirement of narrow band transmitting for harmonic signal extraction and even in the case of broadband transmitting where fundamental and harmonic components overlap, the harmonic component can be extracted. However, even for this approach, the practical application is limited only to wide bandwidth transducers with a bandwidth close to 100% while the standard linear array probes have rather smaller bandwidth, not exceeding 60-70%.

Nowicki and Wójcik [9] proposed a novel method termed Multitone Nonlinear Coding that through the utilizing of the nonlinear acoustic properties of tissue can improve ultrasound image resolution and signal to noise ratio for a mechanical index (MI) lower than for the PI method. PI was considered as a reference method.

2. SHEAR WAVE ELASTOGRAPHY

The propagation of the pressure wave is accompanied by two phenomena - radiation pressure and mass flow, called streaming [10], [11].

The radiation pressure Π is given by

$$\Pi = -\frac{1}{2}\rho_0 v^2 \quad (1)$$

The spatial intensity of the wave in the medium is equal to the energy E included in a cuboid with a unit basis and the height equal to c (speed of sound in the medium),

$$I = E c = \frac{1}{2}\rho_0 c v^2 \quad (2)$$

Comparing (1) and (2) we obtain the relationship between the pressure and the intensity of the radiation

$$\Pi = \frac{I}{c} = E \quad (3)$$

Radiation pressure has a component in the direction of wave propagation, and in contrast to the scalar hydrostatic pressure field is a tensor. As shown [12], the average rate of change of momentum $\langle \frac{d(mv)}{dt} \rangle$ in the medium is numerically equal to the average pressure $\langle p \rangle = \frac{1}{2} \rho v^2$ and hence the radiation pressure is equal to the rate of flow of momentum through a unit surface.

In an infinite homogeneous medium the effect of radiation pressure is not observed, while in a medium whose density varies, energy density varies as well and radiation pressure gradient occurs, if the absorbing medium wave intensity decreases according to the relation

$$I(x) = I_0 e^{-2\alpha x}, \quad (4)$$

where α is the attenuation coefficient. The energy density gradient along the propagation path is given by the formula

$$\frac{dE}{dx} = \frac{1}{c} \frac{dI(x)}{dx}, \quad (5)$$

and finally

$$\frac{d\Pi}{dx} = -2\alpha \frac{I(x)}{c}. \quad (6)$$

For the plain wave, the body force (N/m^3), called *RADIATION FORCE*, may be presented as:

$$F = \frac{W}{c} = \frac{2\alpha I_{ta}}{c} \quad (7)$$

where I_{ta} is the time average intensity at a given space point.

The radiation force with full absorption equals approximately $7 \cdot 10^{-4} \text{NW}^{-1}$. For example: for a complete absorption of waves in water or tissue of $W=1\text{W}$, we obtain F of approximately 0.7mN - a force similar to the force of gravity acting upon the mass weighting 70mg .

The possibility of remote generation of the shear wave was demonstrated by Sarvazyan [13]. The shear wave is produced by strongly concentrated ultrasounds. Bercoff [14], [15] showed that propagation velocity of a shear wave can be determined from the 2D images acquired with a high Frame Rate FR.

Shear wave velocity in tissues constitutes approximately several meters per second and when we assume a fully elastic medium, the shear modulus and velocity are related according to the formula:

$$\mu = \rho c^2 \quad (8)$$

This assumption is also relevant for a viscous and elastic model if the dispersion introduced by viscosity is negligible. In soft tissues, $\nu \gg \omega$ and Young's modulus E may be determined in the approximation:

$$E \approx 3\mu = 3\rho c^2 \quad (9)$$

It has been demonstrated in experimental studies that the shear wave produced by radiation force depends on the viscous and elastic properties of tissue.

The additional effect is related to the radiation pressure gradient and thus the radiation force, producing a constant flow of medium [11].

Tjøtta [16] proposed a simple formula for the speed of streaming being proportional to the absorption coefficient α , the width of the beam $2a$ and field intensity I_0 and inversely proportional to the viscosity η of the medium and the speed of sound in the medium c .

$$v = -\frac{2\alpha I_0 a^2}{\eta c} \quad (10)$$

3. IMAGING WITH AN ADDITIONAL PULSE

All effects mentioned above are rather small for the ultrasonic intensities applied in diagnostic ultrasonography. We are proposing a novel approach combining the propagation of two phenomena, and the compression and rarefaction of the tissue simultaneously with the probing/imaging pulse.

The propagating wave is the sum of two individual pulses differing in frequency by a factor of 5 up to 10 times transmitted coherently in a sequence of two independent transmissions, as shown in fig.1. In the first transmission the high frequency probing pulse coincides with the maximum of compression (displacement) caused by the low frequency wave. Secondly the low frequency wave is shifted by 180 degrees, which results in the change of compression to rarefaction.

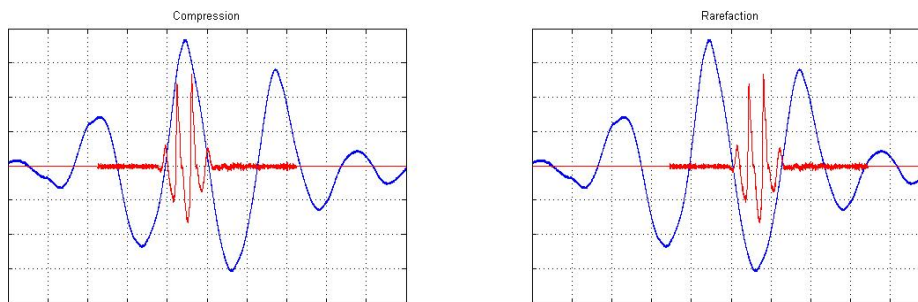


Fig. 1. The actual sequence of transmitted pulses measured with a needle hydrophone. Propagating pulse with compression (left) and rarefaction (right).

It is assumed that during transmissions, tissue is modified in terms of its mechanical properties which influences local acoustic impedance and scattering characteristics. The examination is based on comparing the back-scattered echoes from two subsequent transmissions. Although, as mentioned before, tissue displacements are considered small, the gradients of displacements are large enough. The difference of echoes measures the physical impact of the low frequency pressure wave on tissue and related to local stiffness.

4. ACQUISITION

The imaging system shown in fig. 2 consists of two transducers. An imaging spherical transducer (Vermon, Inc.) with an operating frequency of 7MHz was placed at the opening of a concave transducer (H-102, Sonic Concepts, Inc.) with a lower operating frequency of 1,1MHz. Both transducers were transmitting a two-cycle sine wave, but with a different pressure. Imaging pulse peak to peak pressure was 1,87MPa, measured in the focal zone. To ensure compression/rarefaction, the low frequency transducer used a higher peak to peak pressure of 4,6MPa. The pressure distribution of the combined pulse was measured in a water bath using a needle hydrophone. Because of the transducers' geometry a proper combination

is possible only in the focal region over a certain length (around 10 mm) which is our region of interest (ROI). The method was evaluated with a homogeneous 10% polyvinyl alcohol (PVA) tissue mimicking phantom. A mechanical scanning was performed over 20mm length with 0,04mm intervals (50 lines). Three kinds of echoes (RF data) were captured by an oscilloscope with a 0,5GHz sampling frequency. The first is the transmission of the imaging pulse only for reference purposes. Next, two combined pulses, connected respectively with compression and rarefaction caused by the low frequency wave, were transmitted.

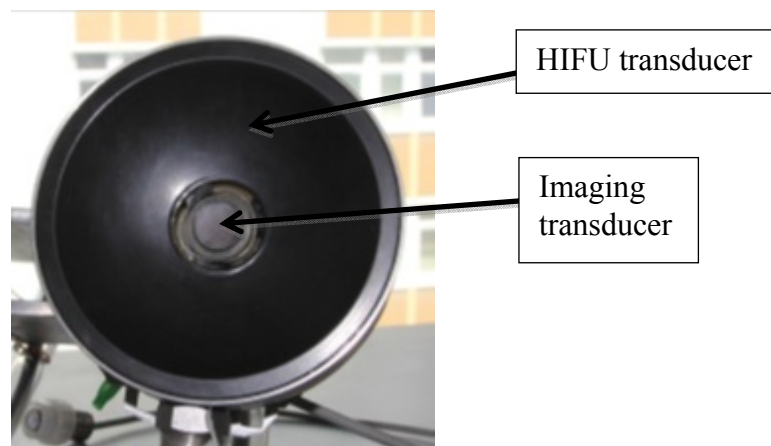


Fig. 2. The imaging system.

5. SIGNAL PROCESSING

Phantom's central region of 35mm height was cropped from the RF data to keep a ROI with only surrounding and removed phantom borders. Our goal was to find a suitable difference between the compression/rarefaction echoes from the ROI and the surrounding region. First, high-pass filtering was appointed to remove low frequency components from the RF data. As will be shown later, even a simple subtraction of the echoes from two subsequent transmissions modifies the ROI. To increase the difference two methods of signal analysis are applied. The first is related to the raw band-pass filtering of subtracted echoes that passes a specific frequency band chosen according to the Gabor transform. Secondly, the wavelet transform of subtracted echoes is performed.

The Gabor transform is the short time Fourier transform with a Gaussian window:

$$Gf(u, \omega) = \int_{-\infty}^{\infty} f(t) e^{-i\omega t} e^{-\pi(t-u)^2} dt. \quad (11)$$

It is designed to analyze frequency content of the signal in the time interval appointed by u . Here it will be used to find a specific frequency band where a change in subtracted echoes occurs, performing successful filtration.

The second approach concerns wavelets. In contrast to the Fourier transform, wavelets can measure time-frequency variations of the signal at different time scales [17]. A wavelet is a function (often called the mother wavelet) ψ with zero average:

$$\int_{-\infty}^{\infty} \psi(t) dt = 0, \quad (12)$$

where t represents time. It is also normalized, so $\psi = 1$. The idea of the wavelet transform is to decompose the signal being analyzed with wavelets that are dilated with a scale parameter s and translated in time by u :

$$\psi_{u,s}(t) = \frac{1}{\sqrt{s}} \psi\left(\frac{t-u}{s}\right). \quad (13)$$

With such a form of equation normalization, $\int_{-\infty}^{\infty} \psi_{u,s}(t) dt = 1$ is preserved. The continuous wavelet transform (CWT) of the signal $f(t)$ is defined by:

$$Wf(u, s) = \int_{-\infty}^{\infty} f(t) \psi_{u,s}^*(t) dt. \quad (14)$$

The idea is to analyze the subtraction of echoes from the two subsequent transmissions with the CWT and to perform filtration. It is expected that the wavelet coefficients change in the ROI where a beam from the low frequency/high pressure transducer is focused. Keeping significant wavelet transform coefficients will ensure better differentiating and emphasizes the subtracted signal in the ROI. Ultrasound imaging pulses are usually modeled as sine-Gaussian waves. The choice of such a wavelet which will efficiently capture sine-Gaussian wave variations, is indicated. The Morlet wavelet is a good choice since it is composed of a complex exponential and the Gaussian window as shown in fig. 3.

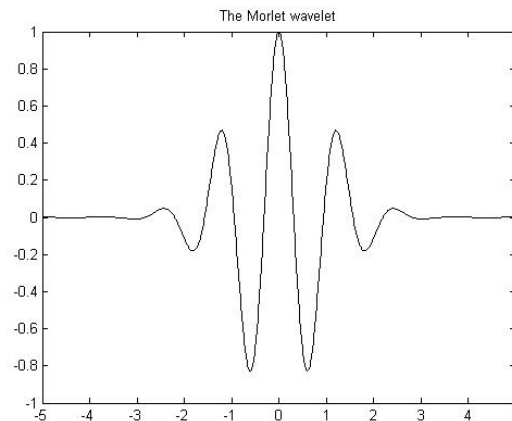


Fig. 3. Example of the Morlet wavelet.

6. RESULTS

As mentioned before, echoes (RF data) were cropped and high-pass filtering was performed in order to remove the low frequency content. Fig. 4 shows an example of echoes for different transmissions. The ROI is situated at a depth between 15 mm and 21.

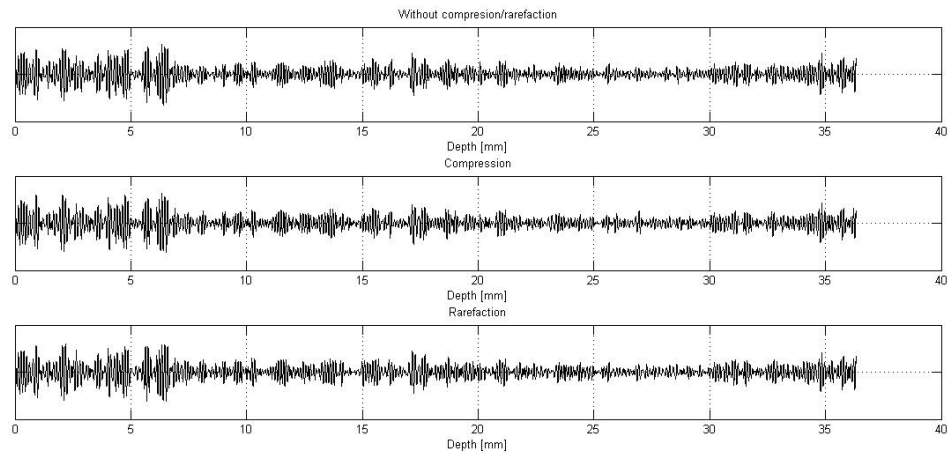


Fig. 4. Echoes from a single transmission: only imaging pulse (upper), imaging pulse plus compression (middle), the imaging pulse plus rarefaction (bottom).

At first sight, no difference in signals can be observed due to the low frequency modulation. Enhancement of the ROI is possible thanks to the subtraction of echoes from compression/rarefaction transmissions as shown below:

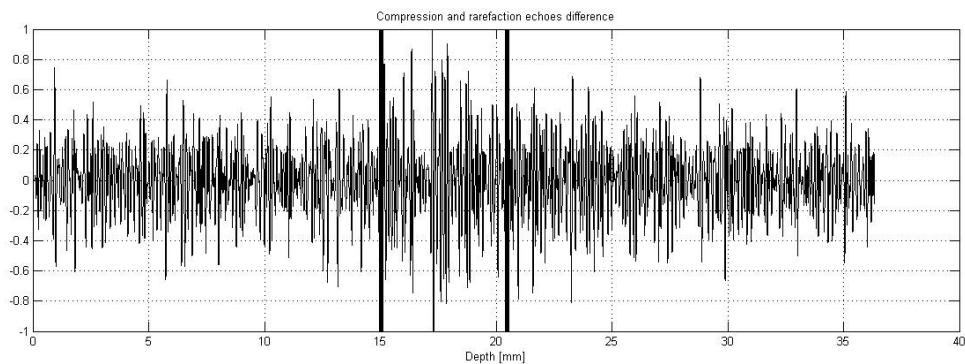


Fig. 5. Subtraction of echoes.

The low level signal's amplitude was normalized to $[-1, 1]$. The difference is more visible if we look at the Gabor Transform of the above signal in fig. 6. One can notice that some Fourier coefficients are greater in the ROI (inside the black frame) and this is the key to successful signal processing. The Butterworth band-pass filter was used to maintain frequencies between 5,5MHz and 7,5MHz, which resulted in a ROI signal improvement (see fig. 7). As would be expected, the subtracted signal is highly sensitive to noise.

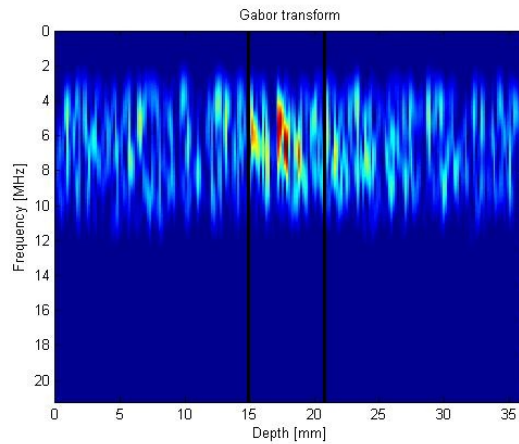


Fig. 6. Gabor transform modulus of subtracted echoes.

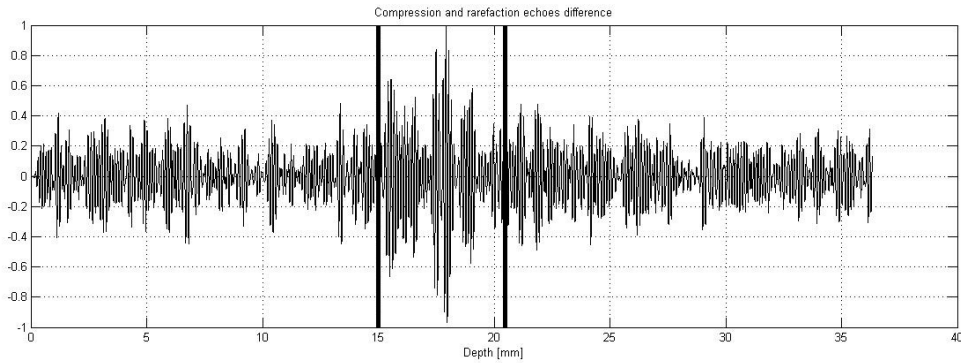


Fig 7. Subtracted echoes after band-pass filtering.

Next, wavelet transform was performed on subtracted echoes:

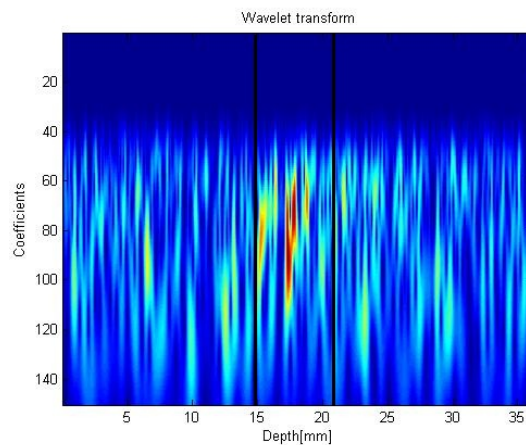


Fig. 8. Wavelet transform modulus of subtracted echoes at normalized scales (sample period equal to one).

Fig. 8 shows that some coefficients are more sensitive to a change in signal due to the compression/rarefaction of the phantom material and these should be preserved. Scales below 60 and above 95 had been reset to 0 and inverse wavelet transform was applied. The subtracted echoes after filtration are shown below:

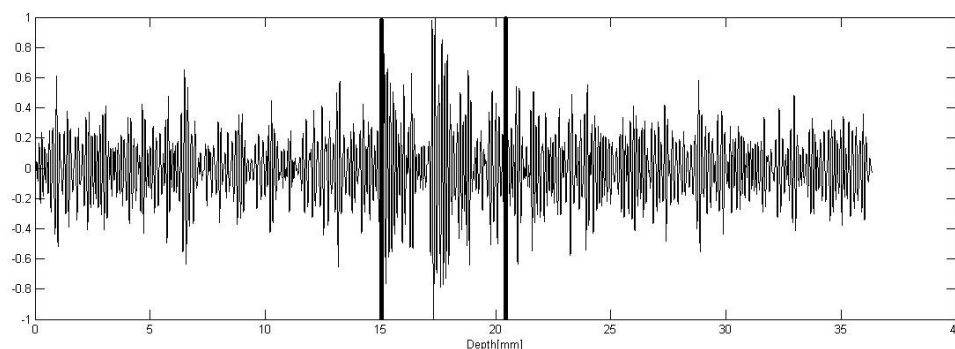


Fig 9. Subtracted echoes after wavelet processing.

Filtration in the wavelet transform domain shows the ability of signal enhancement in the ROI.

All in all, band-pass filtering and wavelet transform were used on each RF line and differential images were reconstructed. After envelope detection, standard and differential images were reconstructed.

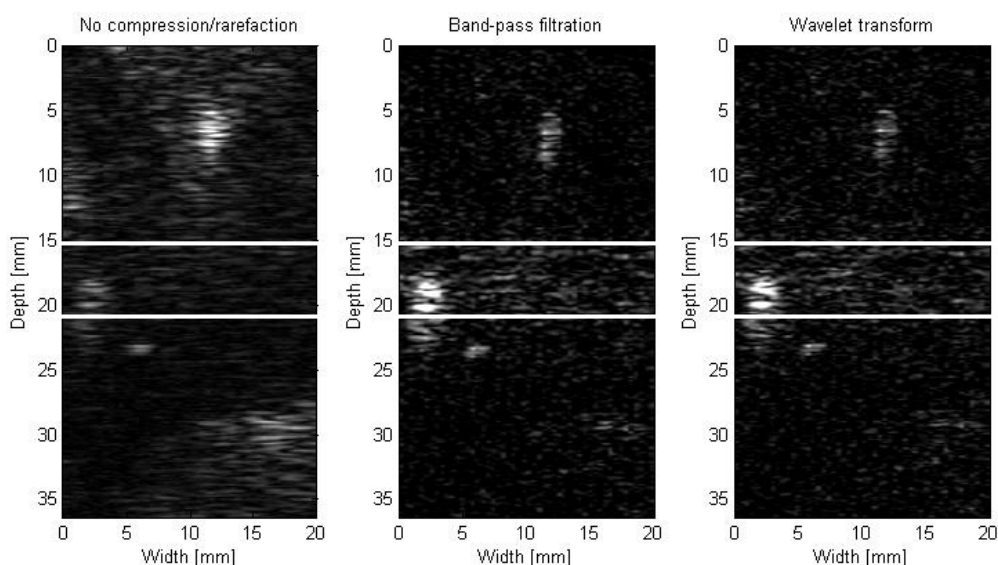


Fig. 10. Standard imaging technique (left), with low frequency wave and: band-pass filtration (mid), wavelet transform coefficients filtration (right), ROI - white frame.

7. CONCLUSIONS

A low frequency wave has a different effect on the scattering of ultrasound within the phantom, depending on its rigidity. Apart from the signal processing we can observe

Fig. 10 shows a standard US image and two differential images obtained with presented methods of which both are capable of detecting changes in backscattered echoes caused by a low frequency pulse. Despite the signal processing approach, it is clearly visible that a comparison of probing pulses results in a change of the image in the ROI. Compression/rarefaction caused by a low frequency wave has an impact on tissue mimicking phantom scattering properties. As expected, the low-frequency wave has less impact on a rigid structure, which translates to smaller differences between compression and rarefaction images resulting in darker final differential images.

REFERENCES

- [1] P.N.T. Wells, H.D. Liang, Medical ultrasound: imaging of soft tissue strain and elasticity, *Journal of the Royal Society Interface*, Vol. 64, 1521-49, 2011.
- [2] M.A. Averkiou, D.R. Roundhill, J.E. Powers, A new imaging technique based on the nonlinear properties of tissues, *Proc. IEEE Ultrason. Symp.*, Vol. 2, 1561-1566, 1997.
- [3] H. Becher, K. Tiemann, C. Pohl, N.C. Nanda, M. A. Averkiou, J. E. Powers, B. Luderitz, Improvement in endocardial border delineation using tissue harmonic imaging, *Echocardiography*, Vol. 15, 511-517, 1998.
- [4] F. Tranquart, N. Grenier, V. Eder, L. Pourcelot, Clinical use of ultrasound tissue harmonic imaging, *Ultrasound Med. Biol.*, Vol. 25, No. 6, 889-894, 1999.
- [5] M.A. Averkiou, Tissue Harmonic ultrasonic imaging, *C. R. Acad. Sci.*, t. 2, Série IV, (Applied physics, Biophysics), 1139-1151, 2001.
- [6] T. Christopher, Finite amplitude distortion-based inhomogeneous pulse echo ultrasonic imaging, *IEEE Trans. Ultrason. Ferr. Freq. Control*, Vol. 44, No. 1, 125-139, 1997.
- [7] T. Christopher, Experimental investigation of finite amplitude distortion-based second harmonic pulse echo ultrasonic imaging, *IEEE Trans. Ultrason. Ferr. Freq. Control*, Vol. 45, No. 1, 158-162, 1998.
- [8] H. D. Simpson, C.T. Chin, P. N. Burns, Pulse inversion doppler: A new method for detecting nonlinear echoes from microbubble contrast agents, *IEEE Trans. Ultrason. Ferr. Freq. Control*, Vol. 46, 372-382, 1999.
- [9] A. Nowicki, J. Wójcik, W. Secomski, Harmonic imaging using Multitone Nonlinear Coding, *Ultrasound Med. Biol.*, Vol. 33, No. 7, 1112-1122, 2007.
- [10] W. L. Nyborg, Acoustic streaming due to attenuating plane waves, *J. Acoust. Soc.*, vol. 25, 68-75, 1953.
- [11] W. L. Nyborg, Acoustic streaming, In Mason, W.P., ed., *Physical acoustics*, IIB, 265-331, 1965.
- [12] T. F. Heuter, R. H. Bolt, *Sonics*, John Wiley and Sons, New York, 1955.
- [13] A. P. Sarvazyan, O. V. Rudenko, S. D. Swanson, J. B. Fowlkes, S. Y. Emelianov, Shear wave elasticity imaging: a new ultrasonic technology in medical diagnosis. *Ultrasound Med. Biol.*, Vol. 24, 1419-1435, 1998.
- [14] J. Bercoff, M. Tanter, M. Fink, Supersonic shear imaging: a new technique for soft tissue elasticity mapping. *IEEE Trans. Ultrason. Ferr. Freq. Control*, Vol. 51, 396-409, 2004.
- [15] J. Bercoff, M. Tanter, M. Muller, M. Fink, The role of viscosity in the impulse diffraction field of elastic waves induced by acoustic radiation force. *IEEE Trans. Ultrason. Ferr. Freq. Control*, Vol. 51, 1523-1536, 2004.
- [16] S. Tjøtta, On some non-linear effects in sound fields, with special emphasis on the generation of vorticity and the formation of streaming patterns, *Arch. Math. Naturvidensk.*, Vol. 55, 1-68, 1959.
- [17] S. Mallat, *Wavelet tour of signal processing*, Elsevier Science, 1999.